Investigation of cutting force components and surface roughness in face milling with different cutting ratios

Csaba Felhő[a*], Frezgi Tesfom[a]

[a] *University of Miskolc*

ABSTRACT

During the face milling process, the choice of technological parameters plays an important role. The two most important parameters are the feed and the depth of cut; the ratio of which is also called the cutting ratio. The main topic of the paper is to examine how different values of the chip ratio affect the components of the cutting force and the roughness of the machined surface. It is also shown how important it is to know the exact geometry of the cutting insert, as well as - in the case of cutting with multiple inserts - the knowledge of the run-out between the individual inserts. Based on the performed investigations, it was determined that the use of a chip ratio close to one is not recommended either in terms of cutting force components or surface roughness.

Keywords: *face milling, cutting ratio, cutting force, surface roughness*

1. Introduction

In the modern advanced manufacturing era, traditional machining equipment are replaced by computer numerical control (CNC) machines for lots of advantage. The most frequently used machining process in the industry gained this advancement are milling and turning processes which are used to remove material from workpieces [1]. Easy machining process, low-cost production system, time and power saving, continuously increase product quality to answer customer demand, and environmentally friendly production system are the main points the manufacturing industry needs to address to compute in the market [2–4]. CNC milling machines are popularly used for metal cutting operations, especially in complicated and very detailed cutting processes [5]. Machines equipped with CNC control are even capable of a certain degree of autonomous operation [6]. Cutting force provided by the spindle and table in different cases greatly affects and is used to predict machining characteristics namely, surface roughness, vibration, chatter, and cutting power.

Face milling, one of the milling cutting methods for creating a planar surface uses a variety of inserts type of material, shape, and numbers to entertain different cutting parameters which affects the surface finish of the product. To increase material removal, high feed rate, depth of cut (increase chip cross-section) [7], and bigger cutting tool diameter are the most responsible cutting parameters. Reducing the thickness of the material to be removed in the design stage is another way of reducing the machining cost if it is observed from the machining time, energy, and tool life perspective. Cutting force components on the workpiece and cutting tool have a direct relationship with these cutting conditions.

The milling machining process is further evaluated by the quality of the workpiece surface finish as it affects its mechanical and other properties [8] in addition to its efficiency. Another very important factor that helps to indicate milling process performance is cutting force to the depth of cut and feed rate [9–11]. Theoretical, numerical, and experiment-based researches are showing promising increases in addressing the demanded minimum production time per workpiece and the minimum cost of production while maintaining the required quality. Such targeted goals can be achieved by using suitable optimized cutting parameters. Face milling uses multiple inserts with round, square, rectangular-shaped, convex triangular, and parallelogram-shaped inserts to remove material from the workpiece [12]. Kundrak et al. [13] studied the effect of milling process parameters such as depth of cut (a_p), cutting speed (v_c) and feed rate (v_f) on the outcome of the face milling process and verified that feed rate is the most dominant factor. This predominant factor requires continuous thrust from the workbench carrying the workpiece against the cutting insert which affects the cutting force. Apart from the feed rate, an increase in the depth of cut raises the contact duration which gives rise to friction between the cutting insert and workpiece. These interconnected effects give a decreased cutting force.

Furthermore, studies of cutting force estimation and its effect on the milling process based on more than one combined cutting parameters effect have been conducted. An experimental investigation on changes in cutting force and surface roughness were conducted by changing the cutting parameters which are depth of cut and feed per tooth [14]. Based on this research, the undeformed chip cross-section variation represented by f_z and ap which stands for feed per tooth and depth of cut respectively influence the power required by the process by altering all three cutting force components. Another research by Akkad and Felhő [15] attested a decreased component of force by decreasing the depth of cut and feed per tooth while the undeformed chip cross-section remains constant. Chirita et al. [16] conducted an experiment designed by response surface methodology and analyzed using ANOVA to study the input parameters (depth of cut and feed) to the mathematical model developed. The inputs, their interactions, and feed direction-cooling interactions had the most significant influence on the main cutting force. The same inputs effect on surface roughness were also studied and the result showed that feed, feed direction, and the interaction of feed direction and cooling type were the most dominant factors.

Modelling the milling process and optimization of the process using numerical solutions with the help of finite element method (FEM) are popular trends in recent research for predicting possible process mechanisms. A new machine learning algorithms approach and finite element analysis were used to predict the cutting force of face milling of AISI 4140 with coated cemented carbide inserts under dry cutting conditions [17]. Different machine learning algorithms were used in the modelling process and ANSYS software was used for the FEM part of the research. From the applied algorithms, SVR achieved the best performance and with this machine learning algorithm, the required cutting

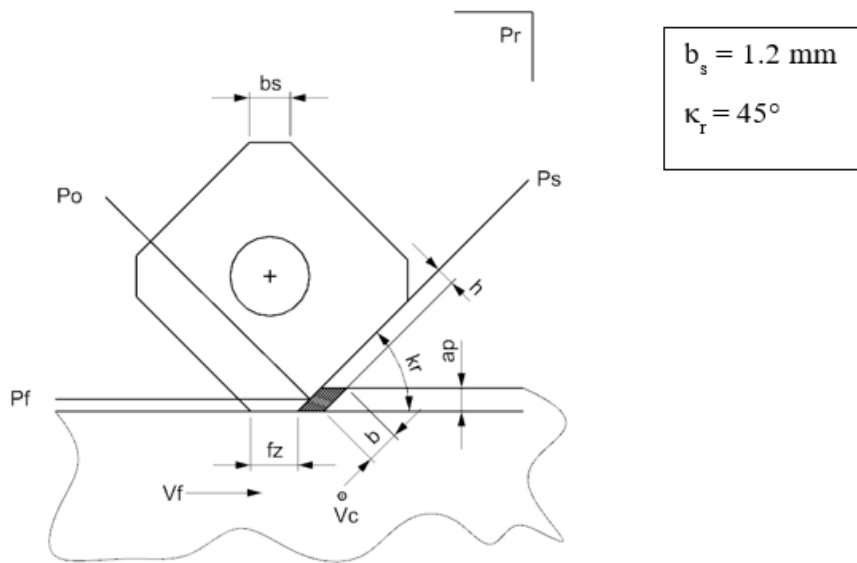**Figure 1.** The applied milling head with the holder

Figure 2. Position of the cutting insert and the workpiece

force during milling procedures was calculated. FEM simulation validated by experiment research on C45 material to study the characteristics of milling with changing cross-sections showed chip ratio equal to one must be avoided from an energy point of view [18]. In the same research, the recommendation given regarding the chip ratio is $a_p/f_z < 1$.

With the brief review done on the conducted research regarding the effect of changing the ratio of the depth of cut and feed per tooth (chip ratio) on cutting force components, it can be concluded that still more research is needed. In the present work, experimental work was conducted to study the varying behaviour of cutting force and surface roughness up on changing ratio of the depth of cut and feed per tooth. This research work can help in selecting the ratio with a minimum cutting force of the two cutting parameters for an optimized machining process.

2. Materials and methods

The experiments were performed on the Perfect Jet MCV-M8 CNC milling machine at the Institute of Manufacturing Sciences of the University of Miskolc. During the experiments, a Canela 0748.90.063 face milling head was used with Dijet SEKN 1203 AFTN JC5030 cutting inserts Fig. 1 shows the applied tool with the holder.

Fig. 2 shows the shape of the cutting insert along with the characteristic geometry and cutting parameters. It can be seen in the figure, that the insert has a 1.2 mm edge parallel to the machined

Table 1. The applied constant parameters

Parameter	Value
Cutting speed, v_c [m/min]	150
Cutter diameter, D_c [mm]	63
Cut width, a_e [mm]	59
Main cutting edge angle, κ_r [°]	45
Wiper edge length, b_s [mm]	1.2
Undeformed chip cross-section, a_c [mm^2]	0.08

Table 2. The applied constant parameters

Workpiece	1	2	3	4	5
Feed per tooth, f_z [mm]	0.01	0.18	0.26	0.32	0.40
Depth of cut, a_p [mm]	0.8	0.44	0.31	0.25	0.20
a_p/f_z ratio, [-]	8.00	2.47	1.18	0.78	0.50
Feed rate (1 insert), v_f [mm/min]	76	136	197	243	303
Feed rate (5 inserts), v_f [mm/min]	379	682	985	1213	1516

surface (b_s, which is often referred to as "wiper edge"), which enables a fine surface roughness to be obtained even with a relatively large feed (when $f_z < b_s$). The representations shown in Fig. 2 are the tool reference plane (P_r), P_s is the tool edge plane, P_f is the assumed work plane and P_o is the orthogonal plane.

In Fig. 2, only the dimensions of the main cutting-edge angle (κ_r), the length of the edge section parallel to the machined surface (b_s), and the cutting speed (v_c) are constant, because, during the test, a different value of the a_p/f_z ratio was selected for each workpiece. Consequently, during cutting, the other parameters changed according to the ratio, which of course influenced the resulting force components. The applied constant parameters are summarized in Table 2 shows the ratio of the feed per tooth and the depth of cut, as well as the values of the feed rates which varies by changing the a_p/f_z ratios in the case of one or five inserts.

When five inserts were placed into the milling head, the axial deviations of the cutting inserts were checked with a Zoller Hyperion tool measuring device. Before the measurement, the inserts were marked with numbers in the milling head to be able to identify them. The axial runout of the inserts in relation to the deepest-lying one (Insert 5) are 37, 25, 49, 20 and 0 μm respectively.

The material of the workpiece used was C45 normalized carbon steel, which is a general-purpose unalloyed steel. Nowadays, it is one of the most widely used raw material to produce various parts (these areas of use can be, for example, parts of the machine and automotive industry that require lower loads, as well as wear-resistant parts, pressure-bearing parts, screw production, etc.). C45 carbon steel is excellent for heat treatment, which is a rather important aspect from the point of view of production technology. Fig. 3 shows the specimen used during the research in a sectional, a top view, and a three-dimensional representation. To carry out the tests, the workpiece had to be made with the dimensions shown in the figure. The holes on the specimen were used for attachment to the dynamometer. The cutting process was performed on the upper 50 × 59 mm surface of the
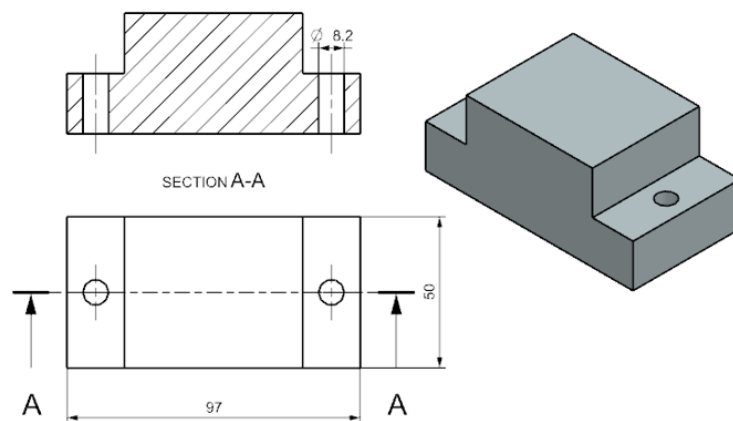

Figure 3. Geometric characteristics of the specimen used during the experiments
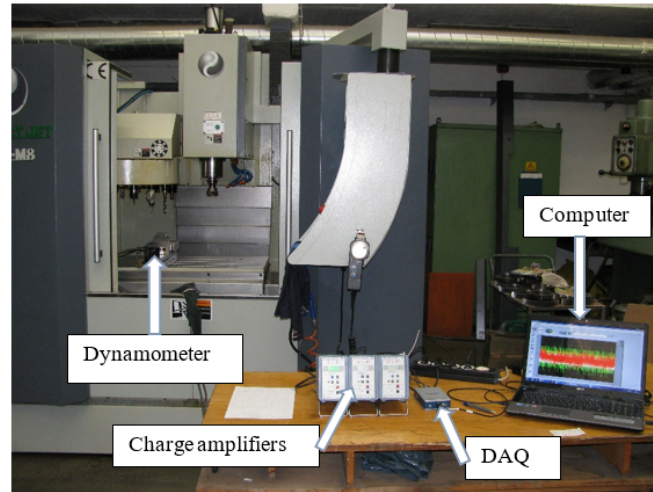
Figure 4. The machining and force measurement system for experimental tests

part. The cutting force components were determined experimentally using instrumental measurements. For this purpose, a force-measuring instrument was attached to the machining system. This force measuring system consisted of a Kistler 9257A three-component dynamometer, 3 pcs Kistler 5011A charge amplifiers, a National Instruments CompactDAQ-9171 four-channel data acquisition unit (USB), and a portable computer for data processing and visualization. The measuring software was created in the LabView programming language. Fig. 4 shows the listed measuring devices assembled in the manner which was necessary to perform the experiments. Roughness measurements were also performed, for which an AltiSurf 520 three-dimensional surface topography analyzer equipment from Altimet Company (France) was used with a CL2 confocal chromatic sensor equipped with an MG140 magnifier. The measurement range of this setup is 300 µm, while its axial resolution is 50 nm. The Altimap software, a product of the Digital Surf company (France), was used to evaluate the roughness data. The measurements and evaluations were performed according to ISO 4287 and ISO 4288 standards because the software of the previously described roughness measuring device supports these standards. However, we would like to note that these standards are already in withdrawn status, the new, current standards are EN ISO 21921-2:2021 and ISO 21920-3:2021, respectively. However, the existence of the new standard does not necessarily mean that instruments according to the old standard can no longer be used for certain tasks. For the three-dimensional parameters, the ISO 25178-2:2021 standard was considered. During the investigations, the following surface roughness parameters were used to qualify the surfaces:

- R_a: arithmetical mean of the absolute ordinate values $Z(x)$ within a sampling length.

- R_z: maximum height of profile: sum of the height of the largest profile peak height Z_p and the largest profile valley depth Z_v within the sampling length. When five sampling lengths are considered (as in the current study), the old ten-point parameter can be obtained.

- S_a: arithmetic mean of the absolute ordinate values within a defined area A.

- S_{10z}: ten-point height of surface: average value of the heights of the five peaks with the largest global peak height added to the average value of the heights of the five pits with the largest global pit height, within the definition area: $S_{10z} = S_{5p} + S_{5v}$.

The microscopic images presented in the article were taken with a Zeiss Stereo Discovery V8-type stereomicroscope.
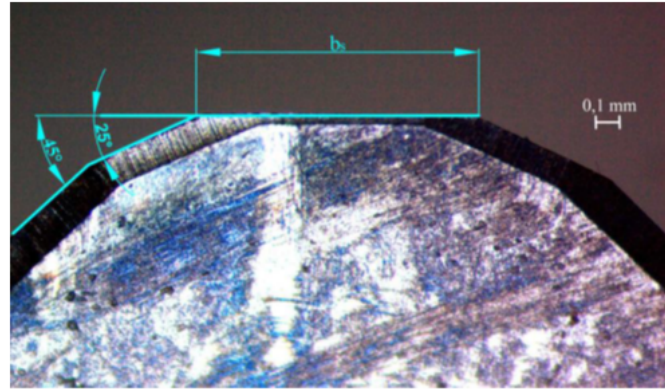
Figure 5. Microscopic image of the working part of the cutting insert

3. Results

During the presentation of the results, it is necessary to first describe an interesting discovery. Even though the insert manufacturer has specified the main cutting-edge placement angle of 45° for the insert, microscopic examinations revealed that it has a 25° facet too (see Fig. 5). It is known that better surface roughness can be achieved with faceted inserts [19]. Such unpublished features help manufacturers make their inserts competitive in the market and possibly outperform other manufacturers' products. However, it is worth noting that the facet also affects the values of the cutting forces, so in the case of applying theoretical calculations and FEM modelling, it is worth examining the inserts carefully in each case, and not relying solely on the public catalogue data. This can be particularly critical when cutting on a micro-scale [20].

Fig. 6 provides help for the interpretation of the individual force components. The applied force-measuring equipment can measure the forces acting on the workpiece since the workpiece has been fixed on the force-measuring cell. These are the forces F_x, F_y, and F_z. At the same time, the forces F_c, F_f, and F_p are the forces acting on the tool, which are directly related to the individual cutting parameters (v_c, v_f and a_p, respectively).
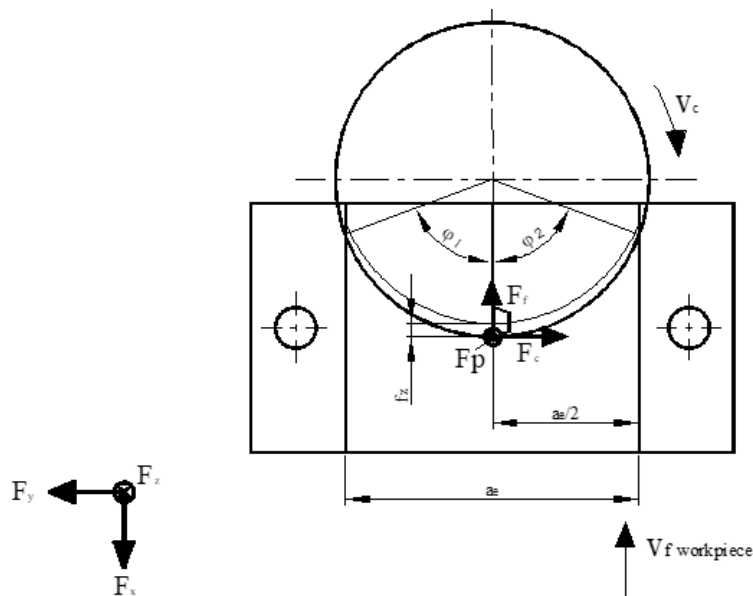

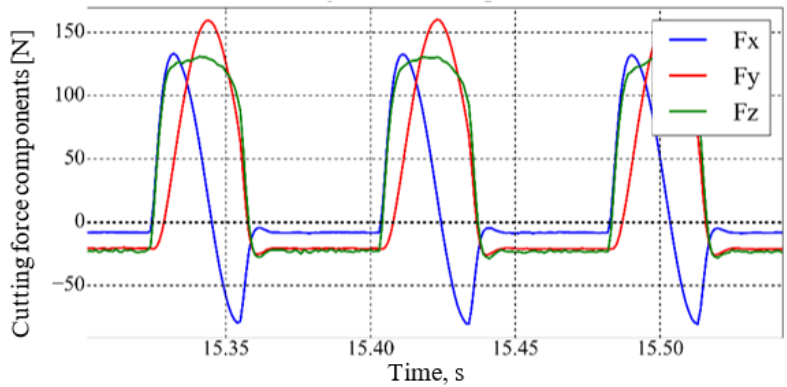**Figure 6.** Interpretation of several cutting parameters and cutting force components

Figure 7. The force components F_x, F_y, F_z when cutting with one insert ($a_p/f_z = 1.18$)

In the following, the results of the cutting experiments with one insert are described. Fig. 7 shows the force components F_x, F_y, F_z for three cutting periods. It can be seen in the figure, that the forces are cyclically repeated as a function of time. It can be also observed, that when no cutting has yet taken place, the zero point of the force components has shifted during the measurement. It was important to take this into account when determining the data, otherwise one can get false values. This can be solved by a simple offset (adding a constant value to the measurement results). Despite all of this, the values of the measured force components can be easily read from the diagram with sufficient accuracy. The periodic pattern of the diagram clearly shows the chip removal stages.

Fig. 8 shows one cutting period of the force components as a function of time, so basically, a single chip removal section is shown enlarged, representing the working period of a cutting edge from the entry to the exit. The diagram in Fig. 8 shows that the force F_y is the largest of the components because the main cutting motion (rotation of the cutter) generates a large force in that direction. The force Fx can also be said to be relatively large, this force is also connected to the main cutting motion and the feeding motion as well. However, there is a change in character for this force component - precisely because of the main cutting speed. From a quarter of the cutting period, the force F_x starts to decrease, and it even goes into the negative range after the insert crossed the milling head centreline, since from here on the main cutting speed has the opposite meaning to the direction of this force. The force F_z shown in the diagram can be said to be relatively linear compared to the other forces, it reaches the linear section in a relatively short time (insert entry time) and drops suddenly at the exit. The components of the cutting force acting on the tool can be deduced in the
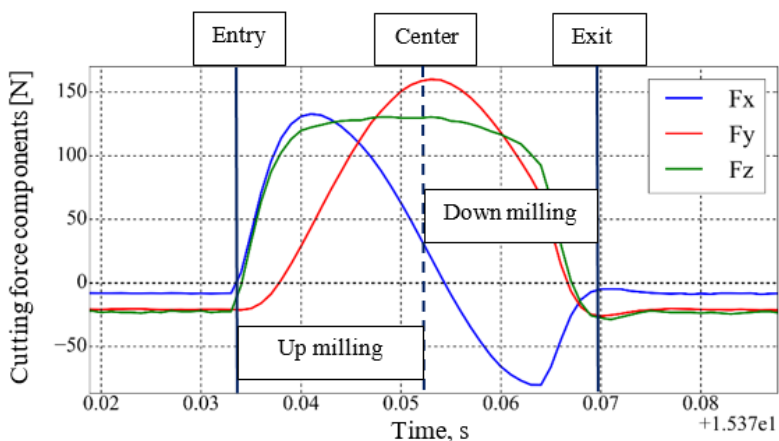

Figure 8. Three characteristic points of the force curves for $a_p/f_z = 1.18$ (cutting with one insert)
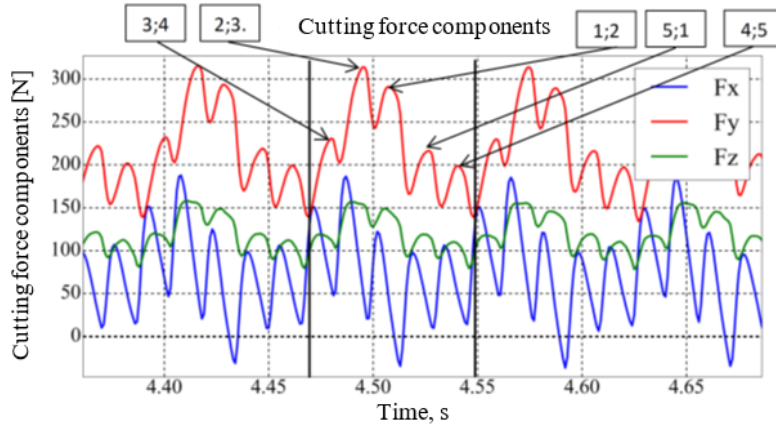
Figure 9. The force components F_x, F_y, F_z measured at cutting with five inserts when ($a_p/f_z = 1.18$)

following way for the cutting insert in a special angular position, as shown earlier in Fig. 6. The main cutting force Fc is obtained when F_y has a maximum, and this occurs at the angular position in Fig. 6: $F_c = F_{y,\text{max}}$. At the same moment, however, the force F_f has only an x-direction component, so $F_f = F_x(F_{y,\text{max}})$. And the force F_p is equal to F_z, the maximum of which was taken.

Fig. 9 shows the force diagram for face milling with five inserts. The diagram shows that even during the cutting of 5 inserts, the shape of the force components is repeated periodically, and they take almost the same value in each period. From the number of peaks of the acting force components, it can be determined that all 5 inserts are indeed cutting during one rotation. The number of inserts simultaneously involved in the cut at a given moment in time (ψ) is given by Eq. (1).

$$\psi = \frac{z_s}{2\pi}(\hat{\varphi}_1 + \hat{\varphi}_2) \approx 1.92, \tag{1}$$

where z_s is the number of inserts, $\hat{\varphi}_1$ is the range of up (conventional) milling and $\hat{\varphi}_2$ is the range of down (climb) milling. The ($\hat{\varphi}_1$) and ($\hat{\varphi}_2$) angles can be determined by Eq. (2) from the diameter of the cutter and the width of the cut as shown in Fig. 10.

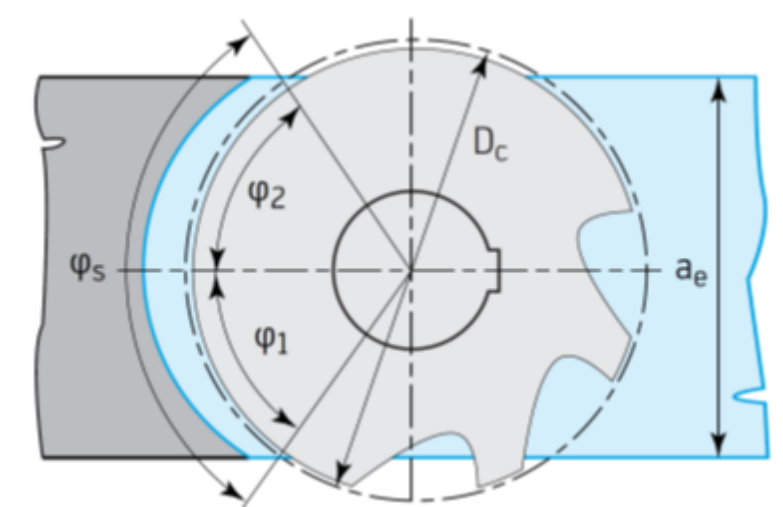$$\hat{\varphi}_1 = \hat{\varphi}_2 = \sin^{-1}\frac{a_e}{D_c} \approx 1.21. \tag{2}$$

Figure 10. Visualization of the $\hat{\varphi}_1$ and $\hat{\varphi}_2$ angles [21]
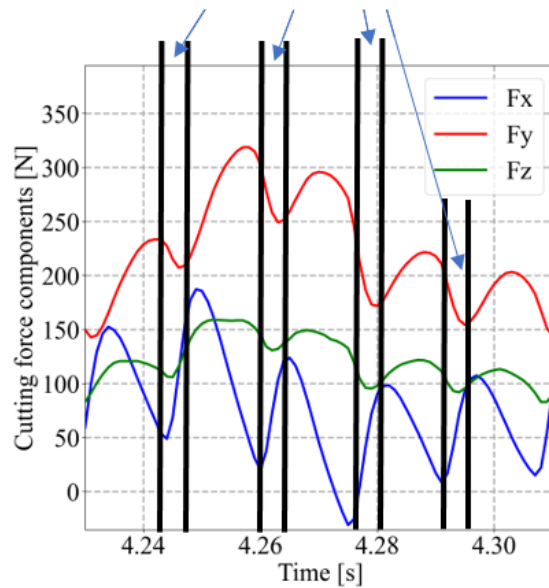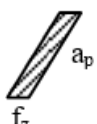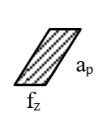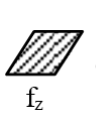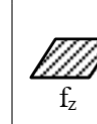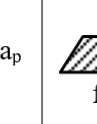
Figure 11. Approximated insert exit and entry ranges according to ψ

From the above value of the number of inserts simultaneously involved in the cut, it can be determined that in this case, two inserts are almost always in cutting action at the same time, only one insert is cutting for a very short time.

These findings for the simultaneously cutting inserts are supported by Fig. 11 (which is, by the way, the enlarged detail of Fig. 10, showing a single cutting period), where it can be seen that the force component F_z decreases at the exit of the currently working insert, and then starts to increase again when the next insert enters into the cut. The other force components - since they depend on

Table 3. Values of the force components measured for face milling with one and five inserts

	Parameter	1	2	3	4	5
Workpiece	Feed per tooth, f_z [mm]	0.10	0.18	0.26	0.32	0.40
	Depth of cut, a_p [mm]	0.80	0.44	0.31	0.25	0.20
	Theoretical chip cross section					
	a_p/f_z ratio	8.00	2.47	1.18	0.78	0.50
1 insert	$F_{x,\mathrm{max}}$ [N]	199.60	163.33	141.34	129.87	120.47
	$F_{y,\mathrm{max}} = F_c$ [N]	234.20	198.82	180.96	174.96	169.42
	$F_{z,\mathrm{max}} = F_p$ [N]	200.10	166.06	153.00	143.67	130.61
	F_f [N]	54.18	35.69	28.05	24.22	23.11
5 inserts	$F_{x,\mathrm{max}}$ [N]	262.4	190.10	178.40	174.60	129.70
	$F_{y,\mathrm{max}} = F_c$ [N]	348.70	291.80	316.70	311.50	217.90
	$F_{z,\mathrm{max}} = F_p$ [N]	160.20	149.90	158.10	162.30	131.20
	F_c [N]	227.06	225.52	253.94	253.54	170.54
	F_f [N]	79.30	51.94	47.32	100.18	34.30

the rotational motion - therefore do not show this change that clearly. The insert exit and entry points indicated in the figure were marked only approximately, based on visual inspections.

Based on Table 3, it is known that the inserts were at distinct height differences from each other in the milling head. From these data, it was concluded that at the highest peaks of force values shown in Fig. 9, the deepest-lying inserts do the cutting, which is the 2nd and 3rd inserts based on Table 3. After the highest force component, the next peak value was formed by the cutting of the 1st and 2nd inserts. The third largest value, and the middle values of the force components, were created by the 3rd and 4th inserts. After that, inserts 5 and 1 followed, and inserts 4 and 5 determined the formation of the smallest peak value at the end of the period.

The cutting force components acting on the tool F_c, F_f, and F_p in the case of cutting with five inserts were determined using the previously described method as well, and the final cutting force values were obtained by averaging the force values of each pair of inserts.

The values of the measured (F_x, F_y and F_z) and inferred (F_c, F_f, F_p) force components for the cutting experiments with one and five inserts are summarized in Table 3. In the case of some force components, the maximum values were taken as numerical values, this is indicated by the "max" subscript. In the following, these parameters are referenced without this index. In the following, the force components F_c, F_f, and F_p acting on the tool will be analysed, as they are generally used to characterize the cutting process.

The diagrammatic representation of the force values is illustrated in Fig. 12. Among the examined force components, F_c is clearly the largest, both in the case of cutting with one insert and with five inserts. However, it is immediately obvious that both the F_c and F_f components have a spike around the $a_p/f_z = 1$ ratio when cutting with five inserts. This leads to the conclusion, that the value $a_p/f_z = 1$ should be avoided, especially when milling with five inserts. By the way, the same jump can also be observed in the F_p diagram belonging to the five inserts, but to a lesser extent.
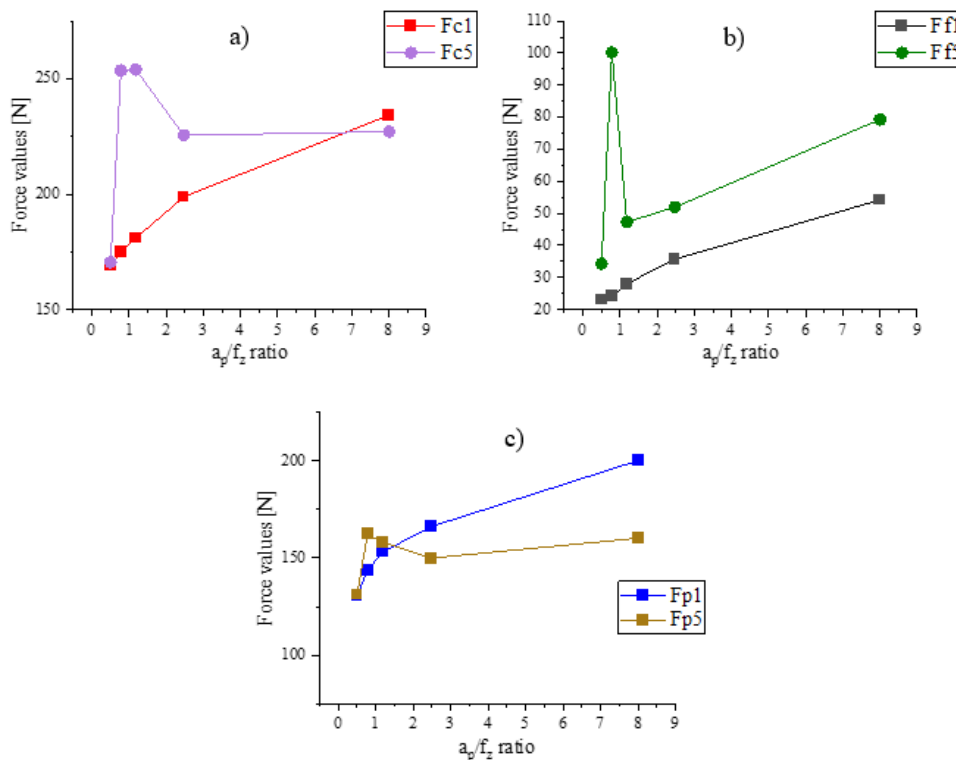

Figure 12. Force components obtained in experiments with one and five inserts (a) F_c; b) F_f; c) F_p)

Table 4. Surface roughness values measured when using one insert

	f_z [mm]	a_p [mm]	R_a [µm]	R_z [µm]	S_a [µm]	S_{10z} [µm]
#1	0.10	0.80	0.25	1.74	0.25	3.16
#2	0.18	0.44	0.48	3.70	0.47	4.00
#3	0.26	0.31	0.54	3.94	0.56	5.26
#4	0.32	0.25	0.57	4.06	0.60	5.21
#5	0.40	0.20	0.62	4.35	0.61	4.37

Table 5. Surface roughness values measured when using five inserts

	f_z [mm]	a_p [mm]	R_a [µm]	R_z [µm]	S_a [µm]	S_{10z} [µm]
#1	0.10	0.80	0.76	5.86	0.95	7.30
#2	0.18	0.44	1.69	11.10	1.71	13.70
#3	0.26	0.31	2.90	16.40	2.77	23.90
#4	0.32	0.25	2.99	14.70	3.35	25.50
#5	0.40	0.20	3.74	23.20	3.59	22.90

Table 4 shows the measured roughness values when cutting with one insert, while Table 5 summarizes the results when five inserts were used in the milling head simultaneously.

Based on the examination of the tabular values, it is quite clear that much higher roughness values were obtained when cutting with five inserts. This is shown even more vividly in the comparison diagrams shown in Fig. 13. It can also be seen from the graphs in Fig. 13, thanks to the high rigidity of the tool and the machine, the high force does not affect the roughness dramatically. However, in the vicinity of the a_p/f_z ratio value of one, the roughness is not favourable, as there is a breaking point on the curves showing the cutting with five inserts (R_{z5} and S_{10z5}).

In the case of all examined 2D and 3D roughness parameters, approximately 3/6-fold increase was observed when five inserts were used compared to the results with a single one. The axial runouts of the inserts were previously described, where the deviations were between 20 and 49 microns. It can be seen that the roughness maxima are smaller even for the smallest run-out. So in most cases, a single insert will actually form the surface topography. The proof of this is shown in Fig. 14: part a) of the figure shows the surface roughness obtained by cutting with one insert, while part b) shows
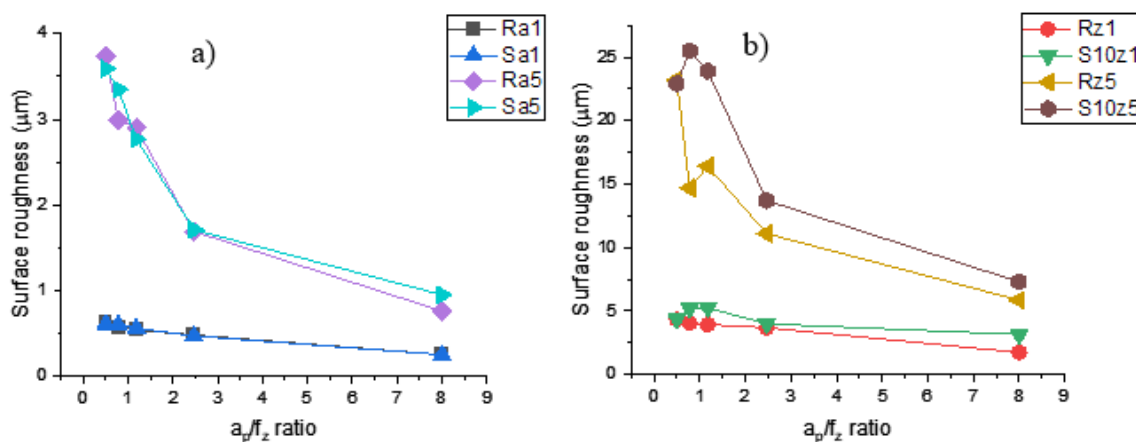

Figure 13. Comparison charts of roughness values (a) R_a and S_a; b) R_z and S_{10z})
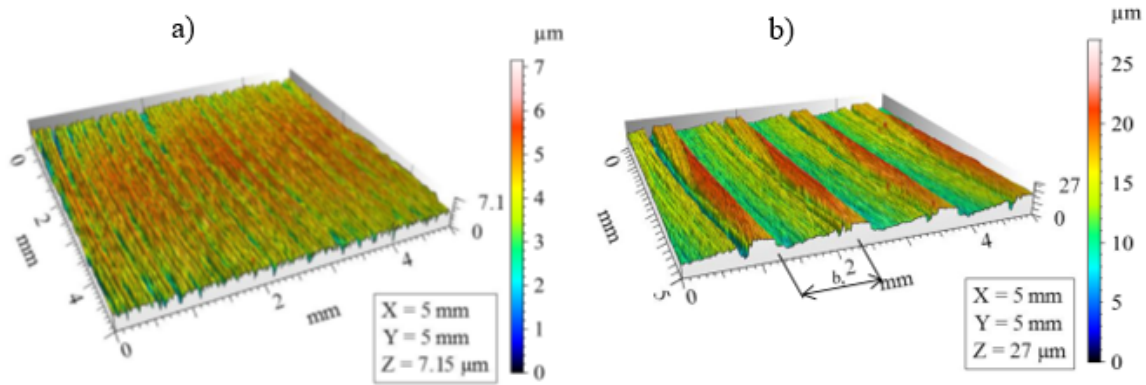
Figure 14. Surface topography images for $f_z = 0.4$ mm (a) one insert; b) five inserts

the result of cutting with five inserts. The figures show the raw measured surfaces for the greatest applied feed value ($f_z = 0.4$ mm) without the use of filters, which is why larger values are visible than in the previous tables.

In Fig. 14, the edge section parallel to the machined surface is also drawn (b_s). Since the value of $b_s = 1.2$ mm, in part a) of the figure, the surface created by the edge roughness of the tool superimposed to the vibrations appears. On the other hand, in part b) of the figure, b_s clearly appears, as well as the repetition period of $f = 2$ mm, so the imprint of a single insert is indeed displayed with the repetition corresponding to the feed per revolution value (f).

4. Conclusions

Based on the tests carried out, the following conclusions were reached:

– First of all, it should be mentioned that during cutting experiments, it is worth examining the tools used from as many points of view as possible, since manufacturers often do not make all detailed information public about their products. Continuous improvements help in the development of better-performing tools, however, in experimental works, especially if the goal is to simulate the process with theoretical or numerical modeling, it is important to strive for an accurate geometrical description of the used tools. In the present work, it was revealed that the insert has a faceted design, which was not disclosed by the manufacturer.

– In the case of face milling with several cutting inserts, the axial run-out of the inserts significantly transforms the forces, often significantly increasing the values of some force components.

– The conclusion regarding the cutting ratio is that the use of the vicinity of the a_p/f_z ratio of 1 is not recommended, especially when using more than one insert, as values of the F_c and F_f force components were the largest here, however it has not affected the surfaces roughness significantly.

5. Acknowledgement

6. References

[1] A. Amiruddin, S. Lubis, *Effectiveness of CNC Turning and CNC milling in machining process*, International Journal of Economic, Technology and Social Sciences 2(2), pp. 575–583, CrossRef

[2] X. Chen, C. Li, Y. Tang, L. Li, Y. Du, L. Li, *Integrated optimization of cutting tool and cutting parameters in face milling for minimizing energy footprint and production time*, Energy 175(15), 2019, pp. 1021–1037, CrossRef

[3] D.Y. Pimenov, A.T. Abbas, M.K. Gupta, I.N. Erdakov, M.S. Soliman, M.M. el Rayes, *Investigations of surface quality and energy consumption associated with costs and material removal rate during face milling of AISI 1045 steel*, International Journal of Advanced Manufacturing Technology 107(7–8), 2020, pp. 3511–3525, CrossRef

[4] A. M. Khan, M. Jamil, K. Salonitis, S. Sarfraz, W. Zhao, N. He, M. Mia, G. Zhao, *Multi-Objective Optimization of Energy Consumption and Surface Quality in Nanofluid SQCL Assisted Face Milling*, Energies 12(4), 2019, p. 710, CrossRef

[5] A. Mgherony, B. Mikó, *The Effect of the Cutting Speed on the Surface Roughness When Ball-End Milling*, Hungarian Journal of Industry and Chemistry 49(2), 2021, CrossRef

[6] R. Benotsmane, L. Dudás, G. Kovács, *The Concept of Autonomous Systems in Industry 4.0*, Advanced Logistic Systems - Theory and Practice 12(1), 2018, pp. 77–87, CrossRef

[7] I. Korkut, M.A. Donertas, *The influence of feed rate and cutting speed on the cutting forces, surface roughness and tool-chip contact length during face milling*, Materials & Design 28(1), 2007, pp. 308–312, CrossRef

[8] B. Rao, C.R. Dandekar, Y.C. Shin, *An experimental and numerical study on the face milling of Ti-6Al-4V alloy: Tool performance and surface integrity*, Journal of Materials Processing Technology 211(2), 2011, pp. 294–304, CrossRef

[9] M.H. Ali, B.A. Khidhir, M.N.M. Ansari, B. Mohamed, *FEM to predict the effect of feed rate on surface roughness with cutting force during face milling of titanium alloy*, HBRC Journal 9(3), 2013, pp. 263–269, CrossRef

[10] Ş. Aykut, M. Gölcü, S. Semiz, H.S. Ergür, *Modeling of cutting forces as function of cutting parameters for face milling of satellite 6 using an artificial neural network*, Journal of Materials Processing Technology 190(1-3), 2007, pp. 199–203, CrossRef

[11] K.A. Abou-El-Hossein, K. Kadirgama, M. Hamdi, K.Y. Benyounis, *Prediction of cutting force in end-milling operation of modified AISI P20 tool steel*, Journal of Materials Processing Technology 182(1–3), 2007, pp. 241–247, CrossRef

[12] N.T. Nguyen, *A development method of cutting force coefficients in face milling process using parallelogram insert*, EUREKA, Physics and Engineering 5, 2021, pp. 36–52, CrossRef

[13] J. Kundrák, A.P. Markopoulos, T. Makkai, N.E. Karkalos, *Effect of Edge Geometry on Cutting Forces in Face Milling with Different Feed Rates*, MManufacturing Technology 19(6), 2019, pp. 984-992, CrossRef

[14] J. Kundrák, K. Gyáni, Cs. Felhő, I. Deszpoth, *The Effect of the Shape of Chip Cross Section on Cutting Force and Roughness when Increasing Feed in Face Milling*, Manufacturing Technology 17(3), 2017, pp. 335-342, CrossRef

[15] M.Z. Akkad, Cs. Felhő, *Effect of Depth of Cut and Feed Rate on the Forces in Face Milling*, Conference: MultiScience - XXXIII. microCAD International Multidisciplinary Scientific Conference 2019, CrossRef

[16] B. Chirita, C. Grigoras, C. Tampu, E. Herghelegiu, *Analysis of cutting forces and surface quality during face milling of a magnesium alloy*, in IOP Conference Series: Materials Science and Engineering 591, 2019, 012006, CrossRef

[17] P. Charalampous, *Prediction of Cutting Forces in Milling Using Machine Learning Algorithms and Finite Element Analysis*, Journal of Materials Engineering and Performance 30(3), 2021, pp. 2002–2013, CrossRef

[18] J. Kundrák, B. Karpuschewski, Z. Pálmai, Cs. Felhő, T. Makkai, D. Borysenko, *The energetic characteristics of milling with changing cross-section in the definition of specific cutting force by FEM method*, CIRP Journal of Manufacturing Science and Technology 32, 2021, pp. 61–69, CrossRef

[19] P. Muthuswamy, *Influence of micro-geometry of wiper facet on the performance of a milling insert: an experimental investigation and validation using numerical simulation*, Sādhanā 47, 2022, p. 140, CrossRef

[20] B.Z. Balázs, M. Takács, *Finite element simulation of micro-milling of hardened tool steel*, IOP Conference Series: Materials Science and Engineering 1246, 2021, 012019, CrossRef

[21] Walter Tools: *Main Catalogue*, 2017, p. 2605